Digest Journal of Nanomaterials and Biostructures Vol. 19, No. 3, July -September 2024, p. 1063 - 1076

Experimental and theoretical study of two Salen-type Schiff bases: green synthesis, characterization, corrosion inhibition efficiency, and biological activity

R. Hadjeb [a,b,*], H. Hamitouche[c], H. Menasra[d]
[a] *Department of Industrial Chemistry, University of Biskra, Biskra, 07000, Algeria*
[b] *Chemical Engineering Laboratory, Blida 1 University, Blida, 09000, Algeria*
[c] *Energy Applications of Hydrogen laboratory, Blida 1 University, Blida, 09000, Algeria*
[d] *Laboratory of Applied Chemistry, University of Biskra, Biskra, Algeria*

As eco-friendly corrosion inhibitors, antioxidants, and antibacterial agents, this study assesses 1,3-bis(2-hydroxybenzylidene) thiourea (B1) and 1,3-bis(2-hydroxybenzylidene) urea (B2), two new Schiff bases, on their performance in these areas. We successfully synthesized these Schiff bases in just 15 minutes using an environmentally friendly approach, and the yield was rather good, ranging from 69.8% to 87.53%. When compared to B2, B1 showed more effective corrosion inhibition and better antioxidant activity. Both chemicals were highly effective against microbes, while B1 was particularly effective against Aspergillus. B. We measured the weight loss to examine the corrosion inhibition impact of XC48 carbon steel in 1M HCl. The findings revealed that at the ideal concentration of 5.10^{-4} M, the estimated IE% of the Schiff bases was 63.8% for B2 and 87.28% for B1. This study employed the Langmuir isotherm model to determine a number of thermodynamic and kinetic characteristics, all of which pointed to a physical adsorbed state. Promising electrical characteristics and robust adsorption on metal surfaces for B1 were corroborated by theoretical investigations employing density functional theory (DFT) and molecular dynamics (MD) simulations. Both the theoretical and practical aspects align with one another.

(Received April 30, 2024; Accepted July 12, 2024)

Keywords: Green synthesis, Schiff base, Biological activity, Corrosion inhibition, Theoretical approaches

1. Introduction

Schiff bases, which are ligands with a wide range of applications in coordination chemistry, are defined by an imine functional group that is generated when an aldehyde and an amine are condensed [1, 2]. They are intriguing prospects for a variety of applications, such as catalysis [3, 4], sensor development [5, 6], and as ligands in metal complexes [7, 8], due to their ease of synthesis, structural diversity [9-11], and tunable electronic and steric properties [12, 13]. Particularly intriguing among the various Schiff bases are those of the salen type, which are tetradentate ligands possessing N2O2 donor sets [14]. Liquids of the Salen type are useful in biomimetic chemistry [15] and catalysis [16] because they conform nearly to the coordination environment of several metalloenzymes.

A major step forward in organic synthesis has been made with the green synthesis of Schiff bases, especially salen types [17, 18]. Conventional synthetic processes frequently employ potentially harmful solvents and chemicals, endangering both the environment and human health [19]. Green synthesis techniques, on the other hand, seek to employ reagents that are less harmful to the environment and safer solvents, if not solvents at all [20-22].These techniques not only adhere to green chemistry principles, but they also frequently produce more pure and abundant products.

Our research here primarily aims at examining the possibility of using two salen-type Schiff bases 1, 3- bis (2-hydroxybenzylidene) thiourea and 1, 3- bis (2-hydroxybenzylidene) urea (which

* Corresponding author: rihana.hadjeb@univ-biskra.dz
https://doi.org/10.15251/DJNB.2024.193.1063

are abreveated B1 and B2 respectively) in corrosion inhibition and antioxidant activities by their green production. Metal corrosion, especially steel corrosion, is a major issue that affects both the economy and public safety. For this reason, it is crucial to find corrosion inhibitors that work. Schiff bases have demonstrated potential as corrosion inhibitors due to their capacity to establish stable complexes with metal ions. Furthermore, Schiff bases have antioxidant characteristics that could help reduce oxidative stress, a factor in many diseases and the aging process.

We hope to shed light on the structure-activity correlations of these Schiff bases by combining experimental and theoretical methods, such as molecular dynamics (MD) simulations and density functional theory (DFT). Insights into their action mechanism and the development of more efficient antioxidants and inhibitors can be facilitated by a better understanding of the molecular foundation of their activity.

2. Experimental

2.1. Preparation of the catalyst

A dry knife was used to slice a fresh lemon. The pieces were subsequently squeezed by hand using a home juicer to obtain the juice. The next step was to strain the juice using a clean cotton cloth that had a pore size of about 100 μm. After that, it was filtered again using filter paper that had a pore size of 20 μm to extract the clear juice by removing solid particles. The succeeding reactions made use of the collected clear juice, which served as a catalyst.

2.2. Green synthesis of two Schiff bases

In different beakers, 0.2 mol of salicylaldehyde and 0.1 mol of either thiourea or urea were measured. One milliliter of catalyst was added to these reaction mixtures. After that, the reaction mixture was left at room temperature to stir for ten to fifteen minutes. At the end of the reaction, a solid product was formed ; following washing with distilled water, it was recrystallized with a small amount of 99.9% ethanol to remove impurities. A BOETIUS PHMK 05 apparatus was used to measure the melting points of the Schiff bases. The sample was observed through the eyepiece until it melted completely, and the device's thermometer provided an instantaneous reading. The compounds 1,3-bis(2-hydroxybenzylidene) thiourea (B1) and 1,3-bis(2-hydroxybenzylidene) urea (B2) were then confirmed using infrared and ultraviolet-visible spectra.

2.3. Antibacterial and antifungal activity

B1 and B2 are two Schiff-base compounds that were created. Each stands for 1,3-bis(2-hydroxybenzylidene) thiourea. We assessed the antibacterial and antifungal activity of these compounds using the agar diffusion method (Muller-Hinton medium) and the disk diffusion method (Sabouraud medium), respectively. Here, the test chemicals were deposited on 9-mm sterile Whatman paper disks that had already been inoculated with the test strain of bacteria or fungus **[23]**. We then placed the disks on top of agar, a solid medium. We used the diameter of the inhibitory zone, measured in millimeters, to interpret the results after incubation for bacteria (24 hours) and fungi (48 hours).

We used two fungal strains, Aspergillus brasiliensis ATCC 16404 and Candida albicans ATCC 10231, and four bacterial strains, Escherichia coli, Bacillus spizizenii, Pseudomonas aeruginosa, and Staphylococcus aureus, to assess the antimicrobial activity.

2.4. Evaluation of antioxidant activity

We used the DPPH assay to find out how effective the antioxidant was. The DPPH (2,2-diphenyl-1-picrylhydrazyl) radical reduction capacity of an antioxidant (AH) is quantified using this approach. Each sample was diluted with 10^{-3} g/mL of ascorbic acid, 0.05 g/mL of compound B1, and 0.15 g/mL of compound B2. Each solution was then added to 0.8 mL of a DPPH radical solution dissolved in methanol, with a volume of 0.2 mL for each. The combination was ready for use after 30 minutes of cover and room temperature. We tested all the made solutions for absorbance at 517 nm. We contrasted the results for each examined product with those for ascorbic acid, which served as a benchmark.

2.5. Study of corrosion inhibition

Here we will test the corrosion-blocking capabilities of our Schiff bases in a 1M HCl solution on XC48-type carbon steel. Gravimetric measurements were employed in this study [24]. In order to understand the mechanism of action of these inhibitors, we computed the thermodynamic parameters K_{ads}, ΔG_{ads}, ΔH_{ads}, and ΔS_{ads}, which pertain to the adsorption and dissolution procedures. Thermodynamic parameters are found by vertically placing, without stirring, steel pieces with dimensions (x, y, z) that resemble parallelepipeds in a corrosive solution. The temperature is kept steady and adjusted as required. The inhibitor concentrations used span a broad range, from 5×10^{-3} mol/L to 10^{-5} mol/L. To perform gravimetric analysis, an object is weighed both before and after being immersed in a caustic solution for a specific duration, with or without an inhibitor.

2.5.1. Quantum chemical calculations

Using Gaussian 09, quantum chemical calculations based on density functional theory (DFT) were used to optimize the molecular structures of the monomeric units of B1 and B2 **[25]**. Our Schiff bases' optimal configuration and associated quantum chemical characteristics were derived using the B3LYP-D3/6-311G(d,p) technique.

2.5.2. Molecular dynamics (MD) simulations

Using the Forcite module of Materials Studio, MD simulations were conducted to explore the B1 adsorption mechanism on the steel surface [26]. In order to construct A (9×9) periodic supercell, the most densely packed and stable plane, the Fe(110) surface, was used **[27]**.

3. Results and discussion

3.1. Characterization of Schiff bases B1 and B2

The characteristics of our synthetic Schiff bases B1 and B2 are summarized in the following table.

Table 1. Physicochemical characteristics of synthetic Schiff bases.

Schiff bases	Time (min)	Yield %	Appearance and Color	Fusion Temperator (K)
1,3-bis (2-hydroxy benzylidène) thiourea (B1)	15	69.8%	White	456.15
1,3-bis (2-hydroxy benzylidène) urea (B2)	15	87.53%	Yellow crystals	403.15

We achieved yields of 69.8% and 87.53%, respectively, in the green synthesis of 1,3-bis(2-hydroxybenzylidene) thiourea (B1) and 1,3-bis(2-hydroxybenzylidene) urea (B2). These outcomes demonstrate how effective our method is, which is based on green chemical principles. Omar H. Al-Obaidi reported a traditional synthesis with a 68% yield in 2 hours [28]. We were able to reduce the synthesis time equal to 15 min and achieve competitive yields by minimizing the use of solvents and favoring natural catalysts, highlighting the efficiency and reduced environmental impact of our method.

We took a close look at the Schiff bases' physical characteristics, including their color, appearance, and melting points. The melting point of B1 is 456.15 K, and it appears as a white solid, whereas the melting point of B2 is 403.15 K, and it shows as yellow crystals. Omar H. Al-Obaidi [28] found comparable tendencies for related compounds, suggesting these features reflect both the compounds' purity and their structural diversity.

3.2. FTIR spectroscopie and UV-visible analysis

In order to validate the structure of the produced chemicals, FTIR spectroscopy was essential. Results obtained in conformity with the literature [29-31] are shown in Fig. 1 and 2 as the hydroxyl groups absorption bands at 3300–3800 cm^{-1} and the azomethine groups bands at 1600 cm^{-1} [32]. Consistent with the findings of S. Deng and F. Bentiss [33, 34], our UV-Vis investigations, as shown in Fig. 3, reveal a strong absorption band between 200 nm and 400 nm, suggesting that the enolic form is predominant. This supports the validity of our results [35].

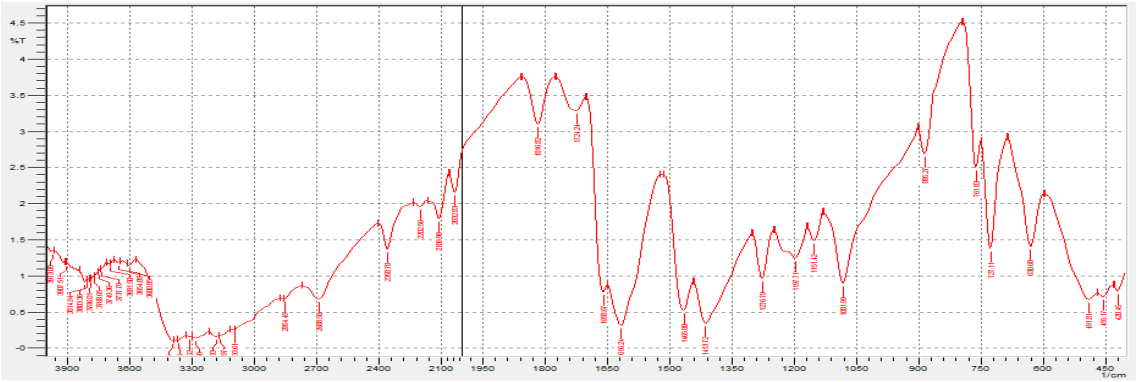

Fig. 1. Infrared spectrum of compound B1.

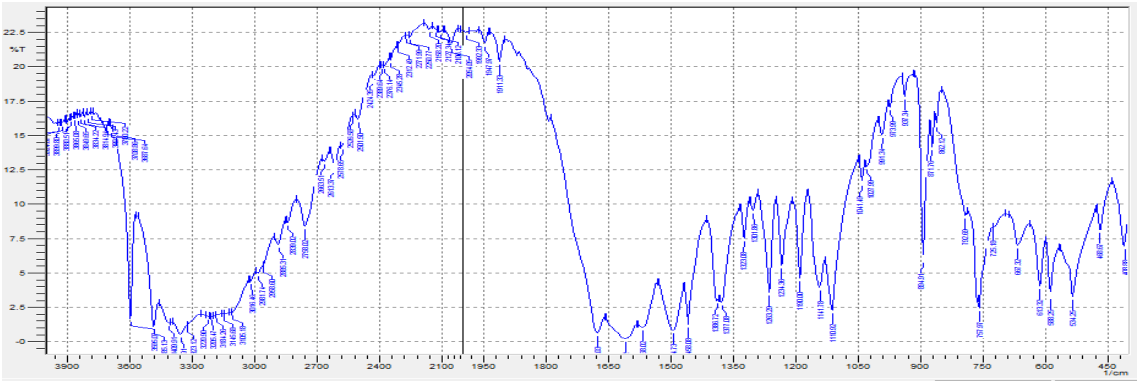

Fig. 2. Infrared spectrum of compound B2.

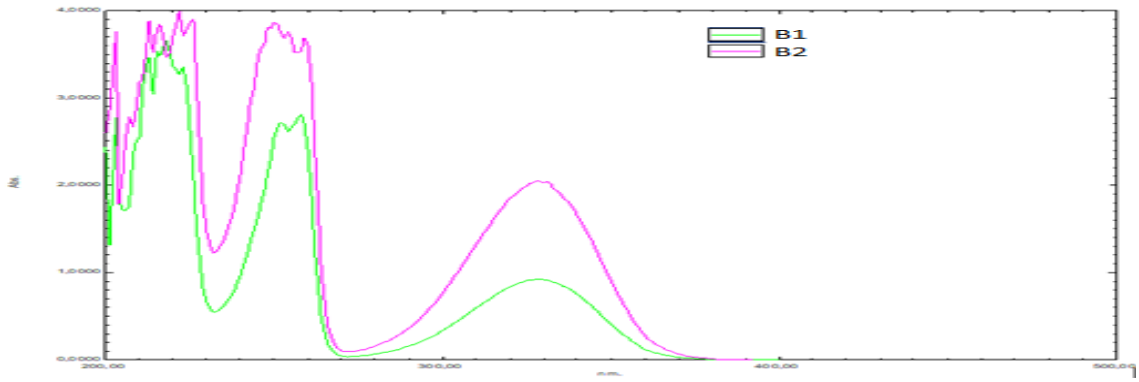

Fig. 3. UV-Vis spectrum of compound B1 and B2 in cyclohexane.

3.3. Antibacterial activity

After 24 hours of incubation at 37°C, the sensitivity was evaluated by measuring the diameter of the inhibitory zones. We compared the synthesized Schiff bases (B1 and B2) at two doses (50 mg/mL and 100 mg/mL) to the antibiotic gentamicin (GN), which served as a positive control. A graduated ruler was used to measure the inhibition zones and find out how big the zone that formed around the 9-mm disk was. Figures 4 to 7 show the findings of the investigation on the antibacterial activity of the Schiff bases.

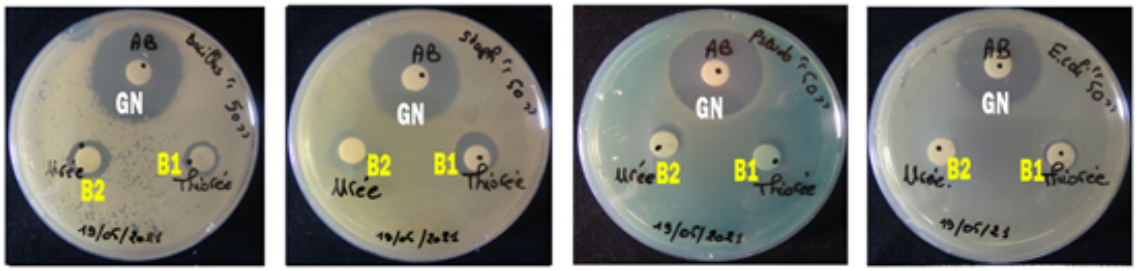

Bacillus Subtilus (+) **Staphylococcus Aereus (+)** **Pseudomonas Aeruginosa (-)** **Escherichia coli (-)**

[B1, B2]= 50 mg/ ml **[GN]= 2 mg/ ml**

Fig. 4. The effect of Schiff bases B1 and B2 on bacterial strains at 50mg/mL.

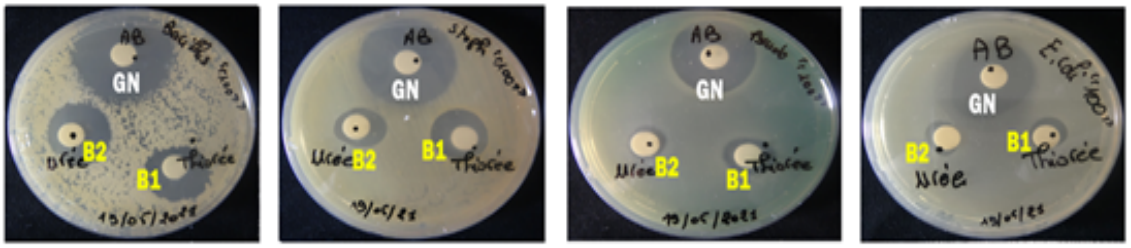

Bacillus Subtilus (+) **Staphylococcus Aereus (+)** **Pseudomonas Aeruginosa (-)** **Escherichia coli (-)**

[B1, B2]= 100 mg/ ml **[GN]= 2 mg/ ml**

Fig. 5. The effect of Schiff bases B1 and B2 on bacterial strains at 100mg/mL.

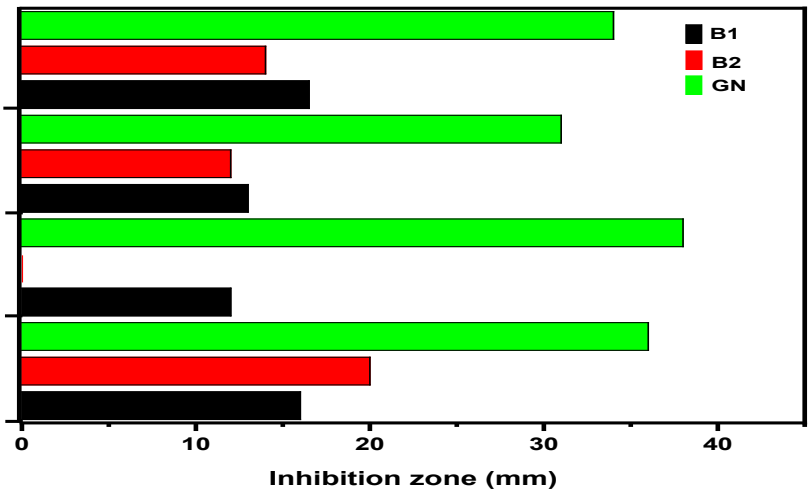

Fig. 6. Antibacterial activity in mm for both Schiff bases at 50 mg/mL.

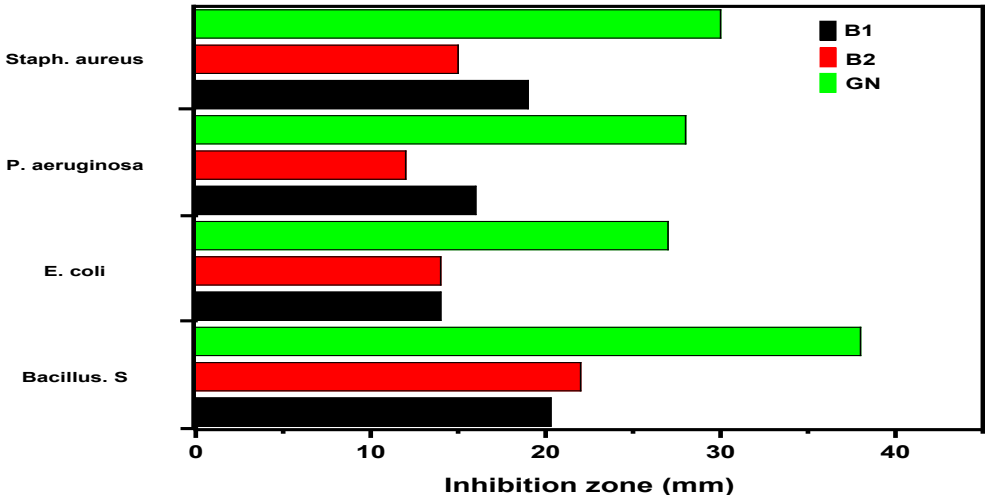

Fig. 7. Antibacterial activity in mm for both Schiff bases at 100 mg/mL.

Findings show that at 50 mg/mL, Schiff base ligands B1 and B2 effectively inhibited the growth of Gram-positive bacteria Bacillus.S and Staph.aureus, respectively, with inhibition zones of 16 mm and 16.5 mm for B1 and 14 mm to 20 mm for B2. With inhibition zones measuring 12–13 mm, they demonstrated poor activity against Gram-negative bacteria P. aeruginosa and E. coli; however, compound B2 failed to demonstrate any antibacterial action against E. coli. However, at 100 mg/mL, it was also shown that all bacteria were significantly reduced in number. While Gram-negative bacteria E. coli and P. aeruginosa showed moderate activity in all of the produced compounds, Gram-positive bacteria Bacillus.S and Staph. aureus showed excellent activity [35].

3.4. Antifungal activity

In order to determine if Schiff bases had any antifungal effects, we compared their results to those of the fungicide fluconazole (FL) in tests conducted on Candida albicans and Aspergillus.B. The inhibition zones' sizes (in mm) and their visual representations are shown in figures 8 and 9, which are provided below.

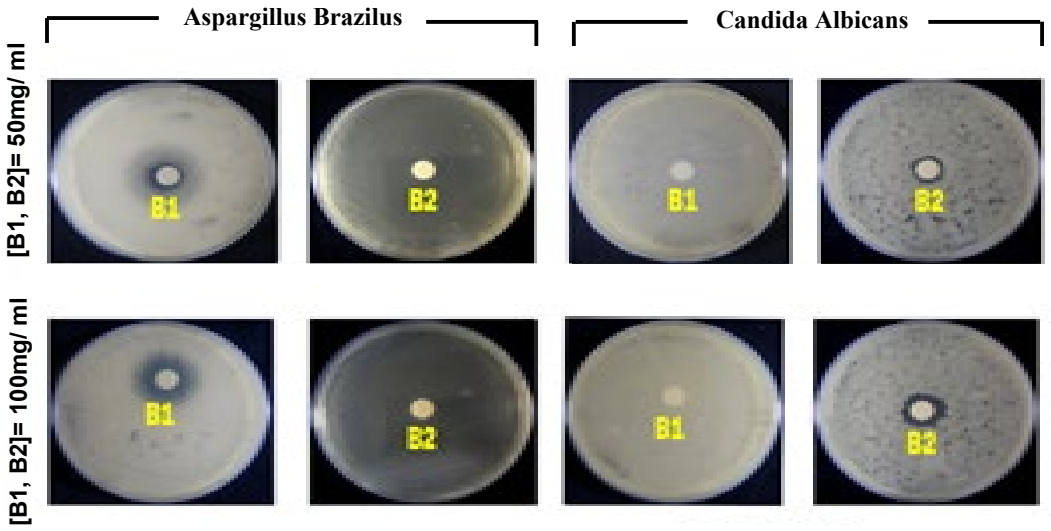

Fig. 8. The antifungal effect of Schiff bases on bacterial strains at 50 and 100 mg/mL.

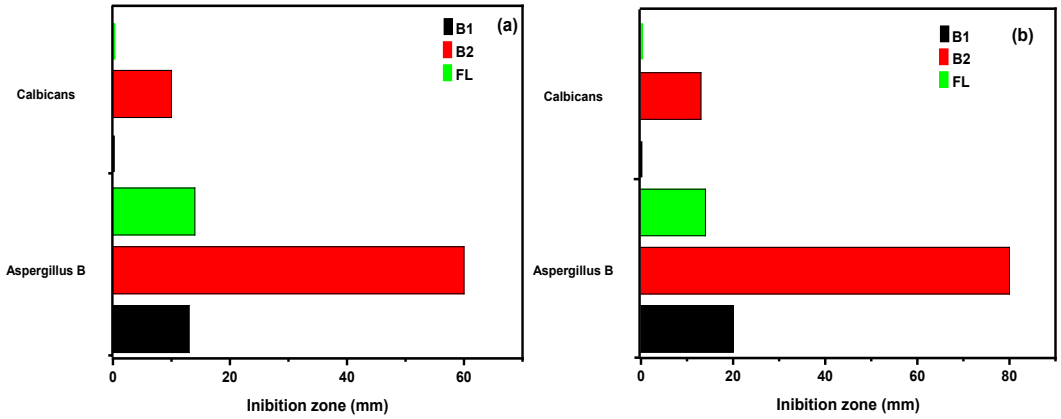

Fig. 9. Antifungal activity in mm for both Schiff bases at, (a) 50 mg/mL (b) 100 mg/mL.

While the fungal strain Aspergillus.B exhibited modest action with a considerably large inhibitory diameter of 14 mm, the antibiotic in this study showed no antifungal activity against the yeast C. albicans. The compound with the strongest antifungal activity was B2, which showed the largest inhibition against Aspergillus.B. At concentrations of 50 mg/mL and 100 mg/mL, the inhibition diameter ranged from 60 mm to 80 mm. Compound B1 was also active, with an inhibition diameter ranging from 13 mm to 20 mm. Findings indicate that compound B2 was highly effective against the Aspergillus fungus, while C. albicans exhibited moderate resistance. The antifungal activity of the compounds was improved by the inclusion of electron-donating groups, as demonstrated in this work [36].

3.5. Antioxidant activity

The results of the antioxidant power of the two Schiff bases, represented in the fig.10 and 11, confirm that better antioxidant activity is observed with compound B1 compared to compound B2.

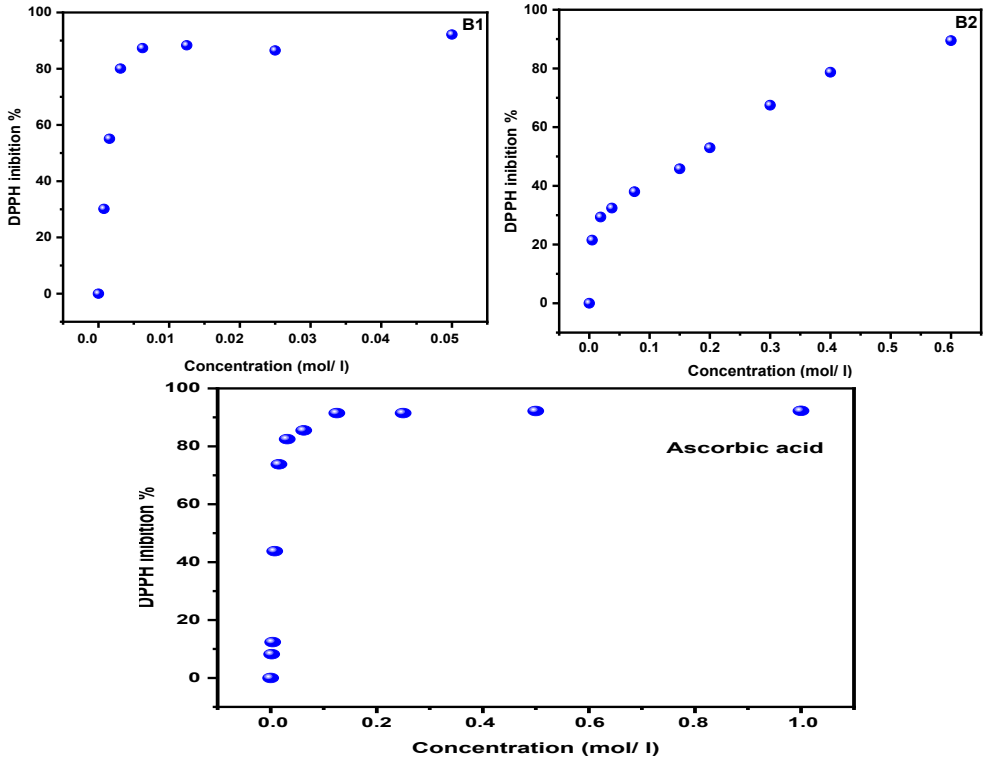

Fig. 10. Percentage of DPPH inhibition (%) of B1, B2 and ascorbic acid.

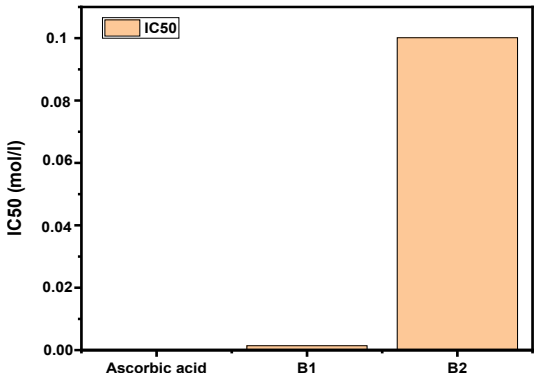

Fig. 11. IC50 values of the tested Schiff bases and ascorbic acid.

All items examined showed a 50% reduction of the DPPH free radical, according to these data. A few examples of IC50 values are ascorbic acid (0.0000506 mol/L), B1 (0.0014021 mol/L), and B2 (0.1001367 mol/L). Compared to Schiff base B2, which exhibited poor antioxidant activity, Schiff base B1 seems to be more effective. One possible explanation for their effectiveness is that they can contribute electrons or hydrogen atoms.

3.6. Weight loss measurements

3.6.1. Effect of inhibitor concentration and immersion time

An inhibitor's inhibitory efficiency is proportional to its concentration. Results for inhibitory efficiency (E%) at varying immersion durations are shown in the table 2.

Table 2. Inhibitory efficiency of corrosion in HCl 1M in the presence of inhibitors at 298K after 1h and 3h.

compound	C(mol/L)	E %	
		After 1h	After 3h
HCL	1M	-	
B 1	10^{-5}	39.05	77.38
	5.10^{-5}	45.20	81.49
	10^{-4}	56.95	83.40
	5.10^{-4}	66.04	87.20
	10^{-3}	58.24	86.85
	5.10^{-3}	60.13	76.15
B2	10^{-5}	25.02	51.07
	5.10^{-5}	28.57	61.40
	10^{-4}	48.13	63.65
	5.10^{-4}	51.02	63.80
	10^{-3}	63.07	68.47
	5.10^{-3}	68.24	72.65

Our Schiff bases prevent steel from corroding in the medium under consideration, as shown in the table. A plausible explanation for this phenomenon is the high rate of Schiff base adsorption on the XC48 carbon steel surface in 1 M HCl. The results show that when the concentration of inhibitors increases, the corrosion rate drops and the inhibitory efficiency increases. As an example, after three hours of immersion, B1 achieves an inhibitory efficiency of 87.28% at a concentration of 5.10^{-4} M while B2 at a concentration of 5.10^{-3} M reaches 72.65%. The data suggests that Schiff base B1 is more stable than B2, as its inhibitory efficacy consistently outperforms B2's, regardless of the immersion period [37-39].

3.6.2. Effect of temperature

We performed a study in the temperature range of 303–333 K for varied inhibitor concentrations throughout 1 hour of immersion using gravimetric measurements to determine the effect of this factor on the evolution of the corrosion rate and inhibitory power of our Schiff bases. The following table displays the corrosion rate (V_{corr}) and inhibitory efficiency (E%) values for each of the Schiff bases that were examined at varied concentrations and temperatures. The data shows that as temperature rises, corrosion rates rise as well, because higher temperatures cause the kinetics of corrosion reactions to speed up.

Table 3. Influence of temperature on the corrosion rate of steel in HCl medium 1 M at different concentrations of inhibitor B1 and B2.

Temperature K	C (mol/L)	B1		B2	
		Corrosion rate ($g/cm^2.h$)	E(%)	Corrosion rate 10^{-3} ($g/cm^2.h$)	E(%)
303	10^{-5}	$2.44.10^{-4}$	38.19	0.920	21.47
	5.10^{-5}	$2.32.10^{-4}$	41.36	0.891	23.89
	10^{-4}	$2.23.10^{-4}$	43.48	0.812	30.67
	5.10^{-4}	$1.69.10^{-4}$	59.71	0.769	34.34
	10^{-3}	$1.61.10^{-4}$	57.18	0.706	39.72
	5.10^{-3}	$1.39.10^{-4}$	64.66	0.638	45.48
313	10^{-5}	$2.27.10^{-3}$	36.87	1.26	9.67
	5.10^{-5}	$4.48.10^{-4}$	39.47	1.23	12.03
	10^{-4}	$4.22.10^{-4}$	42.98	1.22	12.84
	5.10^{-4}	$4.06.10^{-4}$	45.15	1.21	13.67
	10^{-3}	$3.46.10^{-4}$	53.19	1.18	15.40
	5.10^{-3}	$4.08.10^{-4}$	44.92	1.13	18.73
323	10^{-5}	$3.13.10^{-3}$	24.24	2.68	0.51
	5.10^{-5}	$2.77.10^{-3}$	32.84	2.67	0.92
	10^{-4}	$2.76.10^{-3}$	33.21	2.66	1.16
	5.10^{-4}	$2.58.10^{-3}$	37.50	2.60	3.40
	10^{-3}	$2.55.10^{-3}$	38.25	2.58	4.16
	5.10^{-3}	$2.41.10^{-3}$	41.62	2.56	4.76
333	10^{-5}	0.013	21.32	0.920	21.47
	5.10^{-5}	0.013	18.80	0.891	23.89
	10^{-4}	0.014	14.94	0.812	30.67
	5.10^{-4}	0.012	28.33	0.769	34.34
	10^{-3}	0.011	30.79	0.706	39.72
	5.10^{-3}	0.010	36.23	0.638	45.48

3.6.3. Adsorption isotherm and thermodynamic parameters

The adsorption isotherm associated with the inhibitor adsorption process was determined using the coverage rates (θ) for various inhibitor concentrations measured gravimetrically within the temperature range [303–333K]. After extensive testing with other isotherms such as Temkin and Frumkin, we determined that the Langmuir isotherm is the most appropriate adsorption isotherm for both of our Schiff bases [40].

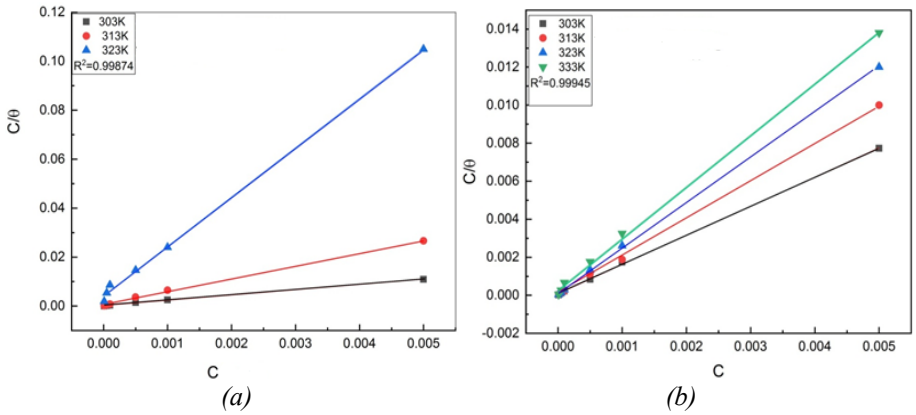

(a) *(b)*

Fig. 12. Langmuir adsorption isotherm of steel in 1M HCl in the presence of B1 (a) and in the presence of B2 (b); at different temperatures.

The linear correlation coefficients are close to 1, as seen in the figures above, suggesting that the adsorption of these Schiff bases on the steel surface in a hydrochloric acid environment followed the Langmuir isotherm model. One may get the adsorption equilibrium constant K_{ads} at any temperature by referring to the Langmuir isotherm. The following equation describes the relationship between K_{ads} and the standard free energy of adsorption, $\Delta G°_{ads}$:

$$\text{It is written as} \qquad K_{ads} = 1/55.5 * \exp(-\Delta G°_{ads}/RT) \tag{1}$$

The water concentration in the solution is 55.5 mol/L [41]. The following equation, derived from the previous relationship, permits us to determine $\Delta G°_{ads}$ for every temperature: $G°_{ads}$ is equal to $H°_{ads}$ minus T times $S°_{ads}$ [42]. The table below summarizes the various thermodynamic properties of our Schiff bases:

Table 4. The K_{ads}, $\Delta G°_{ads}$, $\Delta H°_{ads}$ and $\Delta S°_{ads}$ values of B1and B2 at each temperature value.

T (K)	K_{ads}		$\Delta G°_{ads}$ (j/mol)		$\Delta S°_{ads}$ ($J.mol^{-1}.k^{-1}$)		$\Delta H°_{ads}$ ($kJ.mol^{-1}$)	
	B1	**B2**	**B1**	**B2**	**B1**	**B2**	**B1**	**B2**
303	12897.56	5387.98	-33944.66	-31746.83	-47404.09	-127854.56	37.23	31.54
313	54257.88	1972.69	-38801.87	-30181.14				
323	11198.62	235.29	-35806.10	-25438.04				
333	3507.38		-33702.11					

The durability of the adsorbed double layer on the metal surface and the spontaneity of the adsorption process are shown by the negative value of ΔG°ads. In general, chemisorption involves the transfer of charges between organic molecules and the surface of a metal, and physical adsorption is associated with absolute values of ΔG°ads close to 40 kJ/mol or higher. On the other hand, electrostatic interactions between charged molecules and charged metals are the cause of values close to 20 kJ/mol or lower.

The absolute values of ΔG°ads that have been computed are higher than 20 kJ/mol. According to the letterature , the value of ΔG°ads shows that both physisorption and chemisorption play a part in how the Schiff bases stick to the surface, with physisorption being the more common type [43, 44]. According to the published research, physisorption is indicated by absolute values of ΔH°ads less than 40 kJ/mol, but chemisorption is implied by absolute values near 100 kJ/mol. Given that the absolute values of ΔH°ads that we observed are below 40 kJ/mol, we may infer that the inhibitors have been physically adsorbed onto the surface of the steel [45, 46].

3.7. Calculations in quantum chemistry using the DFT approach

Molecular structure and inhibitory efficiency were optimized using the density-functional theory (DFT) approach. The following graphic (fig. 13) shows the optimized molecular structures and the distribution of the HOMO and LUMO densities of the inhibitors that were investigated. For every inhibitor, the following quantum chemical indices have been computed and are included in Table 5 : E_{HOMO}, E_{LUMO}, ΔE, and the dipole moment (μ).

Table 5. Quantum parameters calculated for the studied inhibitors.

Inhibitor	E_{tot} (eV)	E_{HOMO} (eV)	E_{LUMO} (eV)	ΔE (eV)	μ (Debye)
B1	-1236.95	-5.28	-1.97	3.31	5.20
B2	-24876.9	-6.59	-2.36	4.23	7.48

In general, a strong inhibitory effect is produced when the HOMO energy is large because the molecule is more likely to donate electrons to electron-accepting species that have low-energy empty molecular orbitals [47]. Thus, the electron-donating abilities of these inhibitors are comparable. The energy needed to excite one electron in a molecule is the difference between the energy levels of the lowest and highest energy levels in the molecule, which is sometimes referred to as the gap, or ΔE. The inhibitory efficiency is significantly increased when the value of ΔE is low [48]. The adsorption to the metal surface and inhibitory efficiency are both enhanced by the fact that the Schiff base (B 1) has the lowest ΔE value (3.31 eV). It follows that the results of the experimental weight loss approach are consistent with the results of the theoretical calculations.

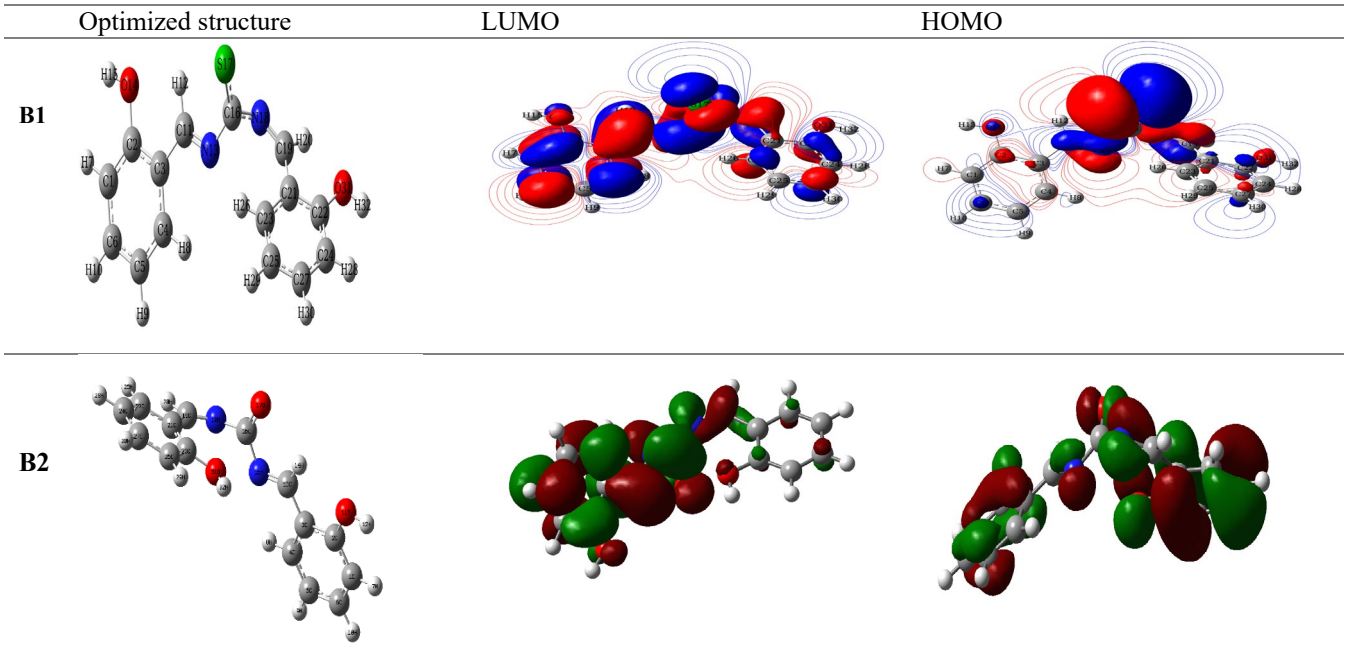

Fig. 13. Optimized molecular structures and distribution of HOMO and LUMO density of inhibitors B1 and B2.

3.8. Simulations using molecular dynamics

The examined surface of Fe (110) displays the equilibrium adsorption configurations of the inhibitory molecule (B1) in Figure 14. Analyzing this image reveals a parallel mode of molecule adsorption on the Fe (110) surface, confirming strong contacts between the molecule and the iron atoms [49]. This mode is relative to the rigid structure of our inhibitor on the steel surface.

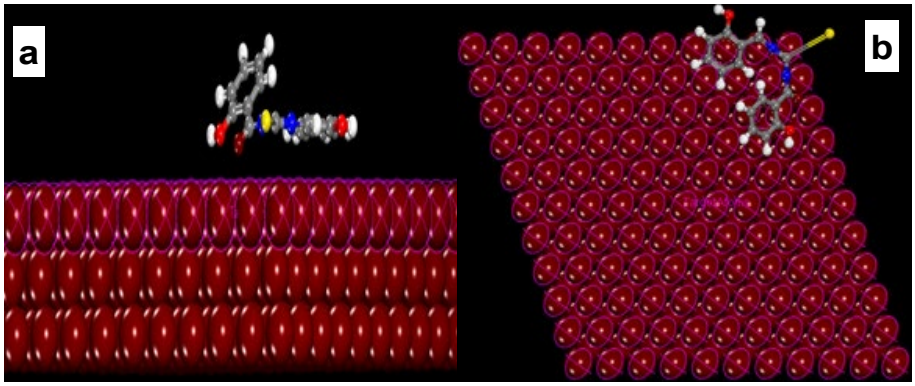

Fig. 14. Equilibrium adsorption configurations of the inhibitory molecule (B1) on the Fe (110) surface: (a) top view and (b) side view.

The different energies of the simulated systems were calculated, and the results obtained are grouped in Table 6. The calculated energies between the studied inhibitory molecules B1 and the Fe (110) surface.

Table 6. The calculated energies between the inhibitory molecule B1 and the surface of Fe (110).

System	Total Energy	Adsorption Energy	Rigid Adsorption Energy	Deformation Energy
Fe (110)	-228,610.5	-969,228.23	-186,604,303.04	-782,623.929

According to the simulation process, the inhibitor B1 provides a large negative adsorption energy [50]. Generally, the high values of adsorption energy obtained explain their higher inhibitory efficiency.

4. Conclusion

This study investigated the antioxidant, corrosion-inhibiting, and antibacterial capabilities of 1,3-bis(2-hydroxybenzylidene) thiourea (B1) and 1,3-bis(2-hydroxybenzylidene) urea (B2), two salen Schiff bases. B1 outperformed the other compounds, showing more antioxidant activity and effectively blocking the acidic corrosion of steel. B1 had strong antifungal effects against Aspergillus.B in addition to its strong antibacterial activity, while B2 showed similar results. Computer models based on molecular dynamics (MD) and density functional theory (DFT) corroborated these results, showing that B1 had good electrical characteristics and strong surface adsorption on metals. According to the findings, B1 has great potential as a versatile agent that can be used for a variety of purposes, which is in line with the objectives of environmentally friendly chemistry.

References

[1] J.E. dos Santos, E.R. Dockal, É.T. Cavalheiro, Carbohydrate polymers, 60 (2005) 277-282; https://doi.org/10.1016/j.carbpol.2004.12.008

[2] A.F. Wady, M.B. Hussein, M.M. Mohammed, Sch. Int. J. Chem. Mater. Sci, 4 (2021) 46-53.

[3] K.C. Gupta, A.K. Sutar, Coordination Chemistry Reviews, 252 (2008) 1420-1450; https://doi.org/10.1016/j.ccr.2007.09.005

[4] V.K. Juyal, A. Pathak, M. Panwar, S.C. Thakuri, O. Prakash, A. Agrwal, V. Nand, Journal of Organometallic Chemistry, (2023) 122825; https://doi.org/10.1016/j.jorganchem.2023.122825

[5] É.N. Oiye, M.F.M. Ribeiro, J.M.T. Katayama, M.C. Tadini, M.A. Balbino, I.C. Eleotério, J. Magalhães, A.S. Castro, R.S.M. Silva, J.W. da Cruz Júnior, Critical Reviews in Analytical Chemistry, 49 (2019) 488-509; https://doi.org/10.1080/10408347.2018.1561242

[6] K.V. Reddy, D. Yuvaraja, J.M. Manriquez, K. Lokesh, M. Amshumali, Reaction Chemistry & Engineering, 7 (2022) 2550-2561; https://doi.org/10.1039/D2RE00193D

[7] T. Ashraf, B. Ali, H. Qayyum, M.S. Haroone, G. Shabbir, Inorganic Chemistry Communications, 150 (2023) 110449; https://doi.org/10.1016/j.inoche.2023.110449

[8] S. Rai, R. Kothari, Digest Journal of Nanomaterials & Biostructures (DJNB), 18 (2023); https://doi.org/10.15251/DJNB.2023.181.31

[9] R. Hadjeb, A. Bara, D. Barkat, MATEC Web of Conferences, EDP Sciences, 2013, pp. 01047; https://doi.org/10.1051/matecconf/20130301047

[10] R. Hadjeb, D. Barkat, Arabian Journal of Chemistry, 10 (2017) S3646-S3651; https://doi.org/10.1016/j.arabjc.2014.04.002

[11] S. Hazra, S. Mohanta, Coordination Chemistry Reviews, 395 (2019) 1-24; https://doi.org/10.1016/j.ccr.2019.05.013

[12] H. Wang, P. Xu, E. Almatrafi, Z. Wang, C. Zhou, T. Xiong, H. Qin, Y. He, H. Yang, Z. Zeng, Environmental Research, 246 (2024) 118200; https://doi.org/10.1016/j.envres.2024.118200

[13] M. Rospenk, I. Król-Starzomska, A. Filarowski, A. Koll, Chemical physics, 287 (2003) 113-124; https://doi.org/10.1016/S0301-0104(02)00983-7

[14] B.K. Vernekar, P.S. Sawant, Results in Chemistry, 6 (2023) 101039; https://doi.org/10.1016/j.rechem.2023.101039

[15] R. Mazzoni, F. Roncaglia, L. Rigamonti, Crystals, 11 (2021) 483; https://doi.org/10.3390/cryst11050483

[16] A. Ghaffari, M. Behzad, M. Pooyan, H.A. Rudbari, G. Bruno, Journal of Molecular Structure, 1063 (2014) 1-7; https://doi.org/10.1016/j.molstruc.2014.01.052

[17] A. Mermer, N. Demirbas, H. Uslu, A. Demirbas, S. Ceylan, Y. Sirin, Journal of Molecular Structure, 1181 (2019) 412-422; https://doi.org/10.1016/j.molstruc.2018.12.114

[18] S. Nagar, S. Raizada, N. Tripathee, Results in Chemistry, (2023) 101153; https://doi.org/10.1016/j.rechem.2023.101153

[19] Q.-U.-A. Sandhu, M. Pervaiz, A. Majid, U. Younas, Z. Saeed, A. Ashraf, R.R.M. Khan, S. Ullah, F. Ali, S. Jelani, Journal of Coordination Chemistry, 76 (2023) 1094-1118; https://doi.org/10.1080/00958972.2023.2226794

[20] B.K. Banik, B.M. Sahoo, B.V.V.R. Kumar, K.C. Panda, J. Jena, M.K. Mahapatra, P. Borah, Molecules, 26 (2021) 1163; https://doi.org/10.3390/molecules26041163

[21] M. Shukla, H. Kulshrashtha, D.S. Seth, Int. J. Mater. Sci, 12 (2017) 71-76.

[22] D. Berra, S. Laouini, B. Benhaoua, M. Ouahrani, D. Berrani, A. Rahal, Digest Journal of Nanomaterials and Biostructures, 13 (2018) 1231-1238.

[23] W. Geary, Coorination Chemistry Reviews, Elsevier publishing company Amsterdam, 1970.

[24] A. Kouache, A. Khelifa, H. Boutoumi, S. Moulay, A. Feghoul, B. Idir, S. Aoudj, Journal of Adhesion Science and Technology, 36 (2022) 988-1016; https://doi.org/10.1080/01694243.2021.1956215

[25] G. Trucks, H. Schlegel, G. Scuseria, M. Robb, J. Cheeseman, G. Scalmani, V. Barone, B. Mennucci, G. Petersson, H. Nakatsuji, Gaussian, Inc., Wallingford CT, (2009).

[26] D.S. Biovia, Biovia Materials Studio 8.0. 100.21, Dassault Systèmes: San Diego, CA, USA, (2014).

[27] S.K. Saha, A. Dutta, P. Ghosh, D. Sukul, P. Banerjee, Physical Chemistry Chemical Physics, 17 (2015) 5679-5690; https://doi.org/10.1039/C4CP05614K

[28] O.H. Al-Obaidi, Synthesis, Journal of Applied Chemistry, 1 (2012) 352-359.

[29] S. Shibata, Angewandte Chemie International Edition in English, 15 (1976) 673-679; https://doi.org/10.1002/anie.197606731
[30] A. Catsch, A.-E. Harmuth-Hoene, D.P. Mellor, The chelation of heavy metals, 1979.
[31] W.J. Geary, Coordination Chemistry Reviews, 7 (1971) 81-122; https://doi.org/10.1016/S0010-8545(00)80009-0
[32] A.A. Ahmed, D.M. Joshua, A.I. Kubo, Chemical Review and Letters, 4 (2021) 171-177.
[33] X. Li, S. Deng, H. Fu, Corrosion science, 53 (2011) 3241-3247; https://doi.org/10.1016/j.corsci.2011.05.068
[34] F. Bentiss, M. Lebrini, M. Lagrenée, Corrosion science, 47 (2005) 2915-2931; https://doi.org/10.1016/j.corsci.2005.05.034
[35] H. Nazır, M. Yıldız, H. Yılmaz, M.N. Tahir, D. Ülkü, Journal of Molecular Structure, 524 (2000) 241-250; https://doi.org/10.1016/S0022-2860(00)00393-8
[36] S. Chandra, D. Jain, A.K. Sharma, P. SharmaMolecules, 14 (2009) 174-190; https://doi.org/10.3390/molecules14010174
[37] N. Dkhireche, M. Galai, Y. El Kacimi, M. Rbaa, M. Ouakki, B. Lakhrissi, M.E. Touhami, Anal. Bioanal. Electrochem. 10 (2018) 111-135.
[38] A. Altalhi, E. Mohammed, S.M. Morsy, N. Negm, Protection of Metals and Physical Chemistry of Surfaces, 57 (2021) 1242-1250; https://doi.org/10.1134/S2070205121060022
[39] K. Dahmani, M. Galai, A. Elhasnaoui, B. Temmar, A. El Hessni, M. Cherkaoui, Der Pharma Chem, 7 (2015) 566.
[40] M. Mobin, M. Basik, M. Shoeb, Applied Surface Science, 469 (2019) 387-403; https://doi.org/10.1016/j.apsusc.2018.11.008
[41] M. Mobin, M. Rizvi, Carbohydrate polymers, 156 (2017) 202-214; https://doi.org/10.1016/j.carbpol.2016.08.066
[42] A. Fawzy, M. Abdallah, I. Zaafarany, S. Ahmed, I. Althagafi, Journal of Molecular Liquids, 265 (2018) 276-291; https://doi.org/10.1016/j.molliq.2018.05.140
[43] M. Mobin, M. Basik, J. Aslam, Journal of Molecular Liquids, 263 (2018) 174-186; https://doi.org/10.1016/j.molliq.2018.04.150
[44] L. Tang, G. Mu, G. Liu, Corrosion science, 45 (2003) 2251-2262; https://doi.org/10.1016/S0010-938X(03)00046-5
[45] K. Zhang, W. Yang, B. Xu, Y. Chen, X. Yin, Y. Liu, H. Zuo, Journal of colloid and interface science, 517 (2018) 52-60; https://doi.org/10.1016/j.jcis.2018.01.092
[46] M. Prabakaran, S.-H. Kim, N. Mugila, V. Hemapriya, K. Parameswari, S. Chitra, I.-M. Chung, Journal of industrial and engineering chemistry, 52 (2017) 235-242; https://doi.org/10.1016/j.jiec.2017.03.052
[47] A.A. Farag, E.A. Mohamed, G.H. Sayed, K.E. Anwer, Journal of Molecular Liquids, 330 (2021) 115705; https://doi.org/10.1016/j.molliq.2021.115705
[48] J. Saranya, F. Benhiba, N. Anusuya, R. Subbiah, A. Zarrouk, S. Chitra, Colloids and Surfaces A: Physicochemical and Engineering Aspects, 603 (2020) 125231; https://doi.org/10.1016/j.colsurfa.2020.125231
[49] H. Fakhry, M. El Faydy, F. Benhiba, T. Laabaissi, M. Bouassiria, M. Allali, B. Lakhrissi, H. Oudda, A. Guenbour, I. Warad, Colloids and Surfaces A: Physicochemical and Engineering Aspects, 610 (2021) 125746; https://doi.org/10.1016/j.colsurfa.2020.125746
[50] H. Hamani, D. Daoud, S. Benabid, T. Douadi, Journal of the Indian Chemical Society, 99 (2022) 100492; https://doi.org/10.1016/j.jics.2022.100492